

# Radio-over-Fiber Transmission Supporting 65536-QAM at 25GHz Band with High-Pass Delta-Sigma Modulation and RF fading Mitigation

Yixiao Zhu<sup>1</sup>, Xiansong Fang<sup>2</sup>, Longjie Yin<sup>1</sup>, Fan Zhang<sup>2</sup>, and Weisheng Hu<sup>1</sup>

<sup>1</sup>State Key Laboratory of Advanced Optical Communication System and Networks, Shanghai Jiao Tong University, Shanghai, 200240, China

<sup>2</sup>State Key Laboratory of Advanced Optical Communication System and Networks, Peking University, Beijing, 100871, China  
[yixiaozhu@sjtu.edu.cn](mailto:yixiaozhu@sjtu.edu.cn), [wshu@sjtu.edu.cn](mailto:wshu@sjtu.edu.cn)

**Abstract:** We experimentally demonstrate radio-over-fiber transmission of 44.4Gb/s 65536-QAM at 25GHz employing 2-bit high-pass delta-sigma modulation. 0.19% EVM is achieved after 10km C-band SSMF transmission, and dispersion-induced RF fading is mitigated by differential skew-enabled spectral shaping.

## 1. Introduction

The fifth generation wireless network (5G) provides three main features including enhanced mobile broadband (eMBB), massive machine type communications (mMTC) and ultra-reliable low latency communications (uRLLC) for emerging services [1]. Since the spectrum resources of sub-6GHz bands are congested, millimeter-wave (MMW) band above 24GHz attracts lots of attentions owing to its abundant bandwidth [2]. Meanwhile, considering the reduction of coverage area, it is necessary to deploy a great amount of radio units (RUs) in centralized radio access network (C-RAN), which leads to the need for simplified RU.

In addition to analog- and digital radio-over-fiber (A/D-RoF) architectures, delta-sigma modulation (DSM) is a promising candidate to connect the central/distributed unit (CU/DU) and RU [3]. By adopting over-sampling and 1/2-bit quantization, the digitized 2/4-level waveform is tolerant to nonlinear distortion with superior sensitivity. The analog band-pass filter-based wireless signal recovery also meets the low-cost requirement. For sub-6GHz band, 4-lane real-time transmission of 3.5Gb/s 256-QAM at 3.5GHz is demonstrated over 20km standard single-mode fiber (SSMF) at 1310nm [4]. Based on 4<sup>th</sup>-order cascaded resonator feedforward (CRFF) structure, LTE 14-carrier aggregation is successfully demonstrated in 5Gb/s on-off keying (OOK) link with bandwidth up to 252MHz and modulation format up to 1024-QAM [5]. For MMW band, real-time 100GS/s DSM is implemented for 4.84Gb/s 64-QAM at 22.75-27.5GHz band, which is enabled by the I/Q interleaving-based up-conversion [6]. In Ref.[7], low-power RoF transmitter is reported for 5.25Gb/s 64-QAM at 28GHz by integrating DSM and parallel electro-absorption modulators (EAMs) on a silicon photonics platform.

Another issue for RoF transmission is the power fading impairment [8] caused by the interaction of fiber dispersion and square-law detection in direct-detection (DD) links, which has more serious impact on MMW band. To cope with the fading effect, feasible solutions are put forward including signal-sideband modulation with IQ modulator [9], parallel intensity-/phase-modulation transmitter [10], polarization modulation with 45° polarizer [11] and so on, which enhances the available bandwidth at the expense of higher hardware complexity.

In this work, we propose and experimentally demonstrate dispersion-tolerant and high-fidelity RoF transmission of 44.4Gb/s 65536-QAM at 25GHz band. By employing 2-bit high-pass DSM, 0.19% error vector magnitude (EVM) or 53.9dB SNR can be achieved after 10km transmission in C-band. The RF power fading is suppressed by vestigial sideband (VSB) spectral shaping enabled by differential time skew without optical filter. The influence of time skew, OSR, modulation format and ROP sensitivity are evaluated, confirming a promising solution for MMW applications.

## 2. Experimental Setup, DSP and Principle

The experimental setup of the DSM and differential skew-enabled MMW transmission system is shown in Fig.1. At the transmitter, the original signal is generated by QAM symbol mapping, 2-times up-sampling and Nyquist shaping using digital root-raised cosine (RRC) filter with 0.1 roll-off. After over-sampling to OSR and digital up-conversion, the signal waveform is fed into a 2-bit high-pass delta-sigma modulator, which is designed in 4<sup>th</sup>-order cascaded feedback (CRFB) topology and the coefficients are optimized according to the OSR. As shown in Fig.1(iii) and 1(iv), the output waveform of DSM has 4 levels and the quantization noise is successfully pushed out of the signal band. Before sending to the arbitrary waveform generator (AWG, Keysight M8194), the waveform is 2-times repeated without pre-equalization to match the sampling rate of 100GSa/s. The digitized waveform from differential outputs of AWG drives the upper- and lower-arm of dual-drive Mach-Zehnder modulator (DDMZM, Fujitsu FTM7937) biased at the quadrature point. The optical carrier is emitted by an external cavity laser (ECL) at 1549.79nm wavelength and 15dBm optical power. In our experiment, differential time skew  $\tau$  is manually introduced onto the

negative output. By this means, an inherent asymmetric transfer function of  $\sin(\pi/4 + \pi/\tau t)$  [12] is produced and thus the signal spectrum can be shaped into VSB without using optical filter.

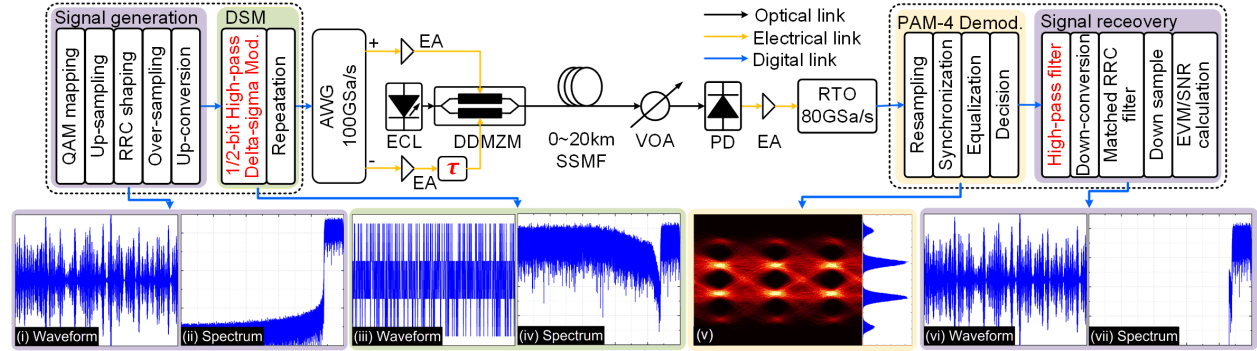


Fig. 1. Experimental setup and DSP stack. AWG: arbitrary waveform generator; EA: electrical amplifier; ECL: external cavity lasers; DDMZM: dual-drive Mach-Zehnder modulator; SSMF: standard single-mode fiber; VOA: variable optical attenuator; PD: photodiode; RTO: real-time oscilloscope. Mod.: modulation; Demod.: demodulation; RRC: root raised cosine.

After 4/10/14/20km SSF transmission, a variable optical attenuator (VOA) is employed for received optical power (ROP) sensitivity measurement. The signal is detected by a photodiode (PD) with 50-GHz bandwidth and subsequently amplified by 50GHz electrical amplifier (EA, SHF S807). The electrical waveform is sampled and stored by a real-time oscilloscope (Keysight DSA-X 96204Q) operating at 80GSa/s for off-line processing. In the receiver-side digital signal processing (DSP), the received waveform is firstly resampled to 2 samples-per-symbol (SPS). After synchronization, the inter-symbol interference (ISI) is eliminated by simplified Volterra equalizer, which has 41 linear taps and 9 2<sup>nd</sup>-order diagonal terms. The eye-diagram after equalization at 2dBm ROP is shown in Fig.1(v), in which the  $\pm 3$  levels have a smaller probability density than  $\pm 1$  levels. For signal recovery, the sequence after decision is shaped by a high-pass filter for out-of-band quantization noise removal as in Fig.1(vii). The filtered waveform in Fig.1(vi) is almost the same as original one in Fig.1(i), indicating high-fidelity transmission of MMW signal. Finally, the sequence is down-converted to baseband, matched filtered, down sampled to 1-SPS, and the EVM/SNR are calculated through  $2^{16}$  symbol samples.

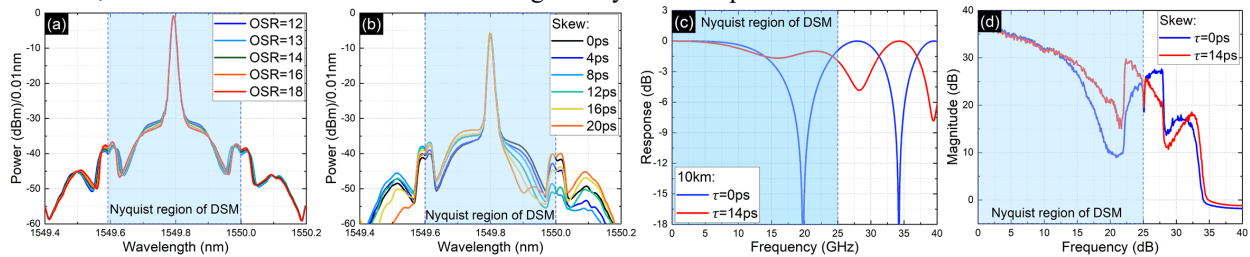


Fig.2. (a) Measured optical spectra with different OSR of DSM. (b) Measured optical spectra with different time skew at OSR of 18. (c) Calculated channel response with skew of 0ps and 14ps after 10km SSF transmission, respectively. (d) Received electrical spectra with 0ps and 14ps differential skew after 10km SSF transmission, respectively.

Fig.2(a) shows the measured optical spectra with OSR varying from 12 to 18 at 0.01 resolution. The differential skew is set as 0ps here. The light blue block is used to represent the Nyquist region of DSM. Since signal bandwidth is inversely proportional to OSR, the quantization noise region around optical carrier becomes wider and the signal region 25GHz (0.2nm) away from carrier gets narrower as the OSR increases. Due to the 2-time repeating operating at the transmitter-side DSP, mirror components are generated outside the Nyquist region, which is also low-pass filtered by the bandwidth of AWG and MZM. Fig.2(b) illustrates the optical spectra with differential skew varying from 0ps to 20ps. We can see that the spectra become asymmetric with right sideband (RSB) suppressed as skew increased to 12ps, and the RSB rises again if skew continues to grow to 20ps. Fig.2(c) plots the theoretical channel response with 0ps and 14ps differential skew, respectively. Thanks to the skew-enabled VSB shaping, the fading notch around 20GHz can be successfully compensated. Moreover, Fig.2(d) compares the received electrical spectra as a validation. With 0ps skew, the spectral components around 20GHz are suppressed, while such fading impairment can be avoided with 14ps skew. The residual loss in high-frequency is caused by the transceiver bandwidth limitation, which can be fully mitigated after equalization and symbol decision as in Fig.1(vii).

### 3. Experimental Results and Discussions

We first evaluate the performance of DSM at different OSRs at 10km as in Fig.3(a). As the OSR increases from 12 to 18, the achieved SNR of recovered signal can be improved from 32.2dB to 54.7dB. According to the SNR/EVM thresholds obtained at requirement of bit-error rate (BER) $<5.9 \times 10^{-3}$ , the highest supported modulation formats are

promoted from 1024-QAM to 65536-QAM. Since various modulation formats exhibit similar SNR under fixed OSR, we investigate the influence of differential skew using 1024-QAM at 10km SSMF as in Fig.3(b) and 3(c). Here the SNR of the 4-level waveform reaches its peak at 14ps skew. Smaller or larger skew values all lead to performance degradation, corresponding to the fading in low/high frequency region. The influence of transmission distance is also measured in Fig.3(d) and 3(e). With 14ps skew, the SNR of the 4-level waveform falls much slower than 0ps configuration, confirming the effectiveness of skew-enabled VSB shaping against RF fading.

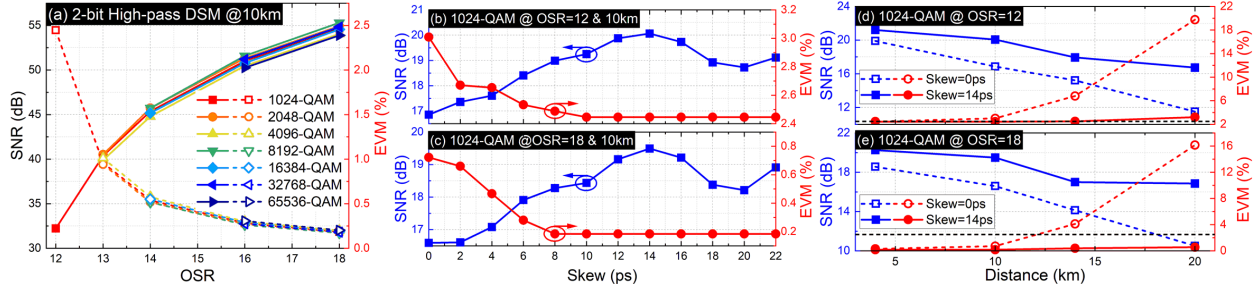


Fig.3. (a) Measured SNR and EVM versus OSR with different modulation formats at 10km SSMF. (b)&(c) Measured SNR of 4-level waveform and EVM of original signal after 10km transmission with OSR of 12 and 18, respectively. (d)&(e) Measured SNR of 4-level waveform and EVM of original signal at different distances with OSR of 12 and 18, respectively.

Furthermore, we measure the ROP sensitivity for different modulation formats at OSR of 18 after 10km SSMF transmission in Fig.4(a)-(d), respectively. SNR ceiling or EVM floor can be reached when ROP is larger than 0dBm, and is thus not presented. At EVM thresholds of 2.5%/1.29%/0.66%/0.34%, -3.0/-2.1/-1.3/-0.5dBm ROP sensitivity is achieved for 1024-/4096-/16384-/65536-QAM, respectively. Fig.4(i)-(iii) illustrate the typical constellations of 1024-, 4096- and 65536-QAM with zoomed view. The constellation points are clearly distinguished.

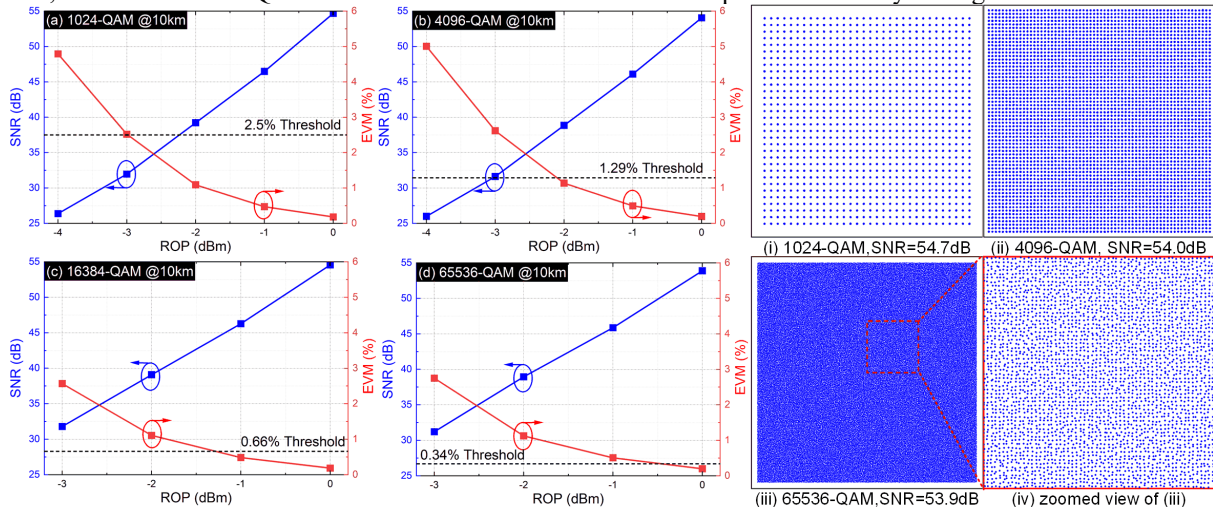


Fig.4. Measured SNR and EVM versus ROP for (a) 1024-QAM (b) 4096-QAM (c) 16384-QAM, and (d) 65536-QAM at OSR of 18 after 10km transmission, respectively. (i)-(iii) Typical constellations of 1024-/4096-/65536-QAM. (iv) Zoomed view of 65536-QAM constellation (iii).

#### 4. Conclusions

In summary, with the help of 2-bit high-pass DSM, we experimentally demonstrate RoF transmission supporting up to 65536-QAM at 25GHz band. For C-band IM-DD link, differential time skew is utilized to mitigate the RF fading without optical filtering. 0.19% EVM or 53.9dB SNR can be achieved after 10km transmission. The impact of OSR, skew, distance and ROP are comprehensively investigated. The proposed scheme offers a cost-effective and promising candidate for MMW applications in 5G/B5G/6G mobile fronthaul.

#### Acknowledgements

This work is supported by National Natural Science Foundation of China (No. 62001287), China Postdoctoral Science Foundation (2021M692098), and National Key R&D Program of China (2018YFB1800904).

#### References

- [1] M. A. Habibi, *et al.*, IEEE Access, **7**, 70371-70421 (2019).
- [2] M. Ptzold, IEEE Vehicular Techn. Magazine, **12**(3), 4-11 (2017).
- [3] L. Breynne, *et al.*, IEEE PTL, **29**(21), 1808-1811 (2017).
- [4] C.-Y. Wu, *et al.*, Proc. ECOC'2018, Tu3B.1.
- [5] J. Wang, *et al.*, IEEE/OSA JLT, **37**(12), 2838-2850 (2019).
- [6] H. Li, *et al.*, IEEE/OSA JLT, **38**(2), 386-393 (2020).
- [7] J. Decelercq, *et al.*, IEEE/OSA JLT, **39**(4), 1125-1131 (2021).
- [8] K. Zhang, *et al.*, OE, **26**(28), 34288-34304 (2018).
- [9] M. Xu, *et al.*, Proc. ECOC'2017, P2.SC8.58.
- [10] S. Ishimura, *et al.*, IEEE/OSA JLT, **36**(8), 1478-1484 (2018).
- [11] S. Liu, *et al.*, IEEE/OSA JLT, **37**(3), 1014-1022 (2019).
- [12] Y. Zhu, *et al.*, OL, **45**(22), 6138-6141 (2020).